ISSN 1970-8734
Vol. 5 N. 1
January 2011

International Review of Mechanical Engineering (IREME)

Contents:

(continued on outside back cover)

Praise Worthy Prize

International Review of Mechanical Engineering (IREME)

The ***International Review of Mechanical Engineering (IREME)*** is a publication of the **Praise Worthy Prize S.r.l..**
The Review is published bimonthly, appearing on the last day of January, March, May, July, September, November.

Published and Printed in Italy by **Praise Worthy Prize S.r.l.,** Naples, January 31, 2011.

Praise Worthy Prize

International Review of Mechanical Engineering (I.RE.M.E.), Vol. 5, N. 1
January 2011

Analysis of Laminar Film Condensation on the Porous Wall of a Vertical Tube

Lazhar Merouani[1], Azeddine Belhamri[2]

Abstract – *A numerical study of laminar film condensation by forced convection of steam-air mixtures in a vertical tube is presented. The internal face of the tube wall is coated with a thin porous layer. A set of complete boundary layer equations governing the conservation of momentum, heat and mass is used to describe the transfers in the liquid film and the mixture. The flow field in the porous medium is described by the Darcy-Brinkman-Forchheimer model. These three phases are related with the continuity of velocity, shear stress, temperature, heat and mass flux at the interfaces. The dimensionless transfer equations are discretized using an implicit finite difference scheme. The liquid film thickness is determined by solving the liquid mass balance equation. Results were obtained for a saturated steam-air mixture. Profiles of velocity, temperature in the three media and vapor mass fraction in the mixture are presented. The effects of main properties of the porous layer such as thickness and Darcy number are highlighted. Additionally, the influence of the inlet Reynolds number and inlet vapor mass fraction of the mixture on the evolution of heat flux and condensate flow rate is also investigated.*

Keywords: *Condensation, Forced Convection, Liquid Film, Porous Layer, Steam-Air Mixture*

Nomenclature

C	Mass fraction of vapor	/
c_p	Specific heat	J kg^{-1} K^{-1}
D	Diffusion coefficient	m^2 s^{-1}
e	Thickness of porous layer	m
F	Forchheimer coefficient	/
g	Gravitational acceleration	m s^{-2}
J_v	Mass flux at the interface l-g	kg m^{-2} s^{-1}
K	Permeability of porous coating	m^2
L_c	Latent heat of condensation	J kg^{-1}
P	Pressure	Pa
q	Mass flow rate	kg s^{-1}
r	Radial coordinate	m
R, R'	Internal and external radius	m
T	Temperature	K
U	Axial velocity	m s^{-1}
V	Radial velocity	m s^{-1}
z	Axial coordinate	m

Greek symbols

α_k	Thermal diffusivity of fluid k	m^2 s^{-1}
δ	Liquid film thickness	m
η_k	Transformed coordinate in fluid k	/
ε	Porosity of porous coating	/
λ	Thermal conductivity	W m^{-1} K^{-1}
μ	Dynamic viscosity	kg m^{-1} s^{-1}
ν	Kinematic viscosity	m^2 s^{-1}
ρ	Density	kg m^{-3}

Dimensionless Parameters

Da	Darcy number	$Da = K/R^2$
Fr	Froude number	$Fr = U_0^2 / Rg$
Ja	Jakob number	$Ja = c_{pl}(T_0 - T_w)/L_c$
Nu	Nusselt number	$Nu = \frac{-R\lambda_e^*}{\Delta T}\left(\frac{\partial T}{\partial r}\right)_w$
Pr_k	Prandtl number of fluid k	$Pr_k = \mu_k c_{pk}/\lambda_k$
Re_0	Inlet Reynolds number	$Re_0 = U_0 R/\nu_0$
Sc	Schmidt number	$Sc = \nu_g/D_v$
ϕ	Total heat flux at the wall between 0 and z	$\phi = \int_0^{z^*} Nu \cdot dz^*$

Subscripts and Superscripts

*	Dimensionless quantity
0	At the inlet ($z = 0$)
c, e	Condensate, effective (porous layer)

Manuscript received and revised December 2010, accepted January 2011

f	End of condensation
g, l, p	Steam-air mixture, liquid film, porous layer
s, v	Saturated vapor, vapor
w	At the wall

I. Introduction

Condensation of vapor on a cooled wall is a process leading to the apparition of liquid droplets or a continuous film flowing on the wall. It is a frequent phenomenon in various fields of industry (steam power plants, refrigeration, heat exchangers, desalination...).

The first theoretical model of condensation has been developed by Nusselt [1] in the case of laminar film condensation of pure saturated vapor on a vertical plate under free convective conditions. The study showed that the heat transfer coefficient decreases along the wall, due to the increased thickness of the liquid film. The presence of the condensate leads to a significant thermal resistance between the vapor and the wall. Many studies have been conducted in order to improve heat transfer by reducing the thickness of the liquid film.

Shekarriz and Plumb [2] examined experimentally the effect of porous fins on film condensation on a horizontal tube. They showed that they are effective in thinning the liquid film and hence enhancing the condensation rate. An alternate method was introduced by Renken et al. [3] for the enhancement of condensation heat transfer within a porous-layer coated surface. Further experimental and modeling work was also performed [4], [5]. The results showed that a highly conductive porous coating may yield a considerable heat transfer enhancement during laminar film condensation under the prescribed conditions.

Ma and Wang [6] presented a numerical study of laminar film condensation on a vertical porous coated plate by including the dispersion effect in the porous coating. The numerical results showed the effects of the porous coating thickness, the effective thermal conductivity and the permeability on condensate film thickness and local Nusselt number. Asbik et al. [7] considered a problem of forced convection condensation in a thin porous layer on a vertical flat plate. An analytical method is developed for the resolution of Darcy-Brinkman-Forchheimer equation used to describe the flow field within the porous medium. Results showed that the film thickness undergoes an important reduction in the case of the Forchheimer term is taken into account. Hence, a better heat transfer is obtained. Additionally, the effects of the porous coating thickness, Reynolds and Darcy numbers are highlighted. Chaynane et al. [8] conducted an analytical and numerical study of laminar film condensation by forced convection of a pure saturated vapor on the porous wall of an inclined plate. The Darcy-Brinkman model is used to describe the flow in the porous layer. They showed that the porous layer contributes significantly to improve the condensation rate. Moreover, the absence of the inertial term in the pure liquid equation leads to an increase of the liquid film thickness. Asbik et al. [9] developed an analytical solution to the problem of condensation by natural convection over a thin porous substrate attached to a cooled impermeable surface. In the porous region, the thermal dispersion is taken into account in the energy equation and the Darcy–Brinkman–Forchheimer model is used to describe the flow. The classical boundary layer equations without inertia and enthalpy terms are used in the condensate region. It is found that due to the thermal dispersion effect, the increasing of heat transfer is significant.

Thus, almost all studies of condensation in porous layers are limited to the case of a pure saturated vapor. Moreover, the transfer equations in the vapor phase are usually neglected. In this work, we consider the problem of laminar film condensation by forced convection of a steam-air mixture in a vertical tube. The tube wall is coated with a thin porous layer. A numerical model is developed taking into account the transfers in the three media (porous coating, liquid film and mixture). The study is carried out by considering some parameters often neglected in studies of condensation in porous media, such as the axial pressure gradient, the inertia and enthalpy terms and the shear stresses at both interfaces (liquid-mixture and liquid-porous layer).

II. Physical Model

The physical model and its coordinate system are shown in Fig. 1. We consider a vertical tube of inner radius R. The internal face of the tube wall is coated with a porous layer of very small thickness e. A steam-air mixture enters the tube with uniform velocity, temperature, vapor mass fraction and pressure. The external face the wall is maintained at a temperature T_w less than the dew point temperature of the mixture. During the fluid flow in the tube, steam condensation leads to the apparition of a thin liquid film flowing on the cooled wall. So, we will consider three distinct regions in the tube: the saturated porous layer, the liquid film and the steam-air mixture. The following simplifying assumptions are adopted:

- Fluids are newtonian, incompressible and flows are laminar,
- Transfers in all phases are steady and two-dimensional,
- Boundary layer approximations are assumed valid for the liquid film and the mixture,
- Physical properties of the three media are assumed constant,
- Temperature of the liquid-mixture interface is equal to the local saturation temperature,
- Pressure is uniform in the radial direction,
- The vapor-gas mixture is supposed to be composed of two ideal gases,

- Heat transfer by radiation and superficial tension effects are assumed negligible,
- The saturated porous layer is homogeneous, isotropic, in local thermodynamic equilibrium with the liquid and completely covered by the condensate.

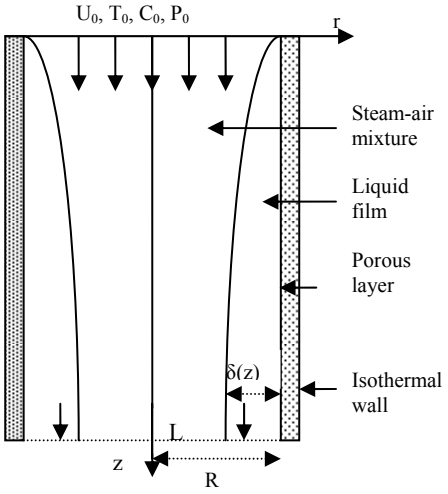

Fig. 1. Physical model

III. Mathematical Formulation

The mathematical model of this problem is described by three domains. In the liquid film and the mixture, transfers are governed by the conservation equations of mass, momentum, energy and diffusion using the classical boundary layer equations. In the porous medium, the flow is described by the Darcy-Brinkman-Forchheimer model which includes the influence of viscous effects, flow inertia and pressure gradient. It is considered as the general flow equation in porous media.

With this formulation and the above assumptions, the governing equations for this problem can be written as follows:

- Porous layer:

$$\frac{\partial U_p}{\partial z}+\frac{1}{r}\frac{\partial\left(rV_p\right)}{\partial r}=0 \tag{1}$$

$$\frac{\rho_l}{\varepsilon^2}\left(U_p\frac{\partial U_p}{\partial z}+V_p\frac{\partial U_p}{\partial r}\right)= =\frac{\mu_e}{r}\frac{\partial}{\partial r}\left(r\frac{\partial U_p}{\partial r}\right)-\frac{dP}{dz}+\rho_l g-\frac{\mu_l U_p}{K}-\frac{\rho_l F U_p^2}{\sqrt{K}} \tag{2}$$

$$\left(\rho c_p\right)_l\left(U_p\frac{\partial T_p}{\partial z}+V_p\frac{\partial T_p}{\partial r}\right)=\frac{\lambda_e}{r}\frac{\partial}{\partial r}\left(r\frac{\partial T_p}{\partial r}\right) \tag{3}$$

- Liquid film (k = l) and mixture (k = g):

$$\frac{\partial U_k}{\partial z}+\frac{1}{r}\frac{\partial\left(rV_k\right)}{\partial r}=0 \tag{4}$$

$$U_k\frac{\partial U_k}{\partial z}+V_k\frac{\partial U_k}{\partial r}=\frac{\nu_k}{r}\frac{\partial}{\partial r}\left(r\frac{\partial U_k}{\partial r}\right)+g-\frac{1}{\rho_k}\frac{dP}{dz} \tag{5}$$

$$U_k\frac{\partial T_k}{\partial z}+V_k\frac{\partial T_k}{\partial r}=\frac{\alpha_k}{r}\frac{\partial}{\partial r}\left(r\frac{\partial T_k}{\partial r}\right)+\xi_k Dc_p^*\frac{\partial T_k}{\partial r}\frac{\partial C}{\partial r} \tag{6}$$

where $\xi_l = 0$ and $\xi_g = 1$,

$$U_g\frac{\partial C}{\partial z}+V_g\frac{\partial C}{\partial r}=\frac{D}{r}\frac{\partial}{\partial r}\left(r\frac{\partial C}{\partial r}\right) \tag{7}$$

The boundary conditions are described below.

At the inlet (z = 0), mixture profiles of velocity, pressure, temperature and vapor concentration are assumed uniform, and the liquid film thickness is zero:

$$U_g=U_0,\quad T_g=T_0,\quad P_g=P_0,\quad C=C_0,\quad \delta_0=0 \tag{8}$$

In the porous layer, the inlet velocity profile is obtained with numerical solution of equation (2) by neglecting the inertia terms and pressure gradient. The inlet temperature profile is obtained with analytical solution of equation (3) without convective terms:

$$T_p\left(r\right)=T_w+\left(T_0-T_w\right)\frac{ln\left(r/R'\right)}{ln\left(R/R'\right)} \tag{9}$$

At the axis of the tube (r = 0), symmetry conditions are considered:

$$\left.\frac{\partial U_g}{\partial r}\right)_0=0,\quad \left.\frac{\partial T_g}{\partial r}\right)_0=0,\quad \left.\frac{\partial C}{\partial r}\right)_0=0 \tag{10}$$

At the liquid-mixture interface ($r_i = R-\delta$), the conditions of continuity of velocity, shear stress, temperature, heat flux, mass flux and local saturation of vapor are imposed using:

$$U_l=U_g,\ \left.\mu_l\frac{\partial U_l}{\partial r}\right)_i=\left.\mu_g\frac{\partial U_g}{\partial r}\right)_i \tag{11}$$

$$T_l=T_g=T_{si},\ \left.-\lambda_l\frac{\partial T_l}{\partial r}\right)_i=J_v L_c-\left.\lambda_g\frac{\partial T_g}{\partial r}\right)_i \tag{12}$$

$$J_v=\rho_l\left(V_l+\left.U_l\frac{d\delta}{dz}\right)_i\right)=\rho_g\left(V_g+\left.U_g\frac{d\delta}{dz}\right)_i\right) \tag{13}$$

At the porous layer-liquid interface ($r = R$), the conditions of continuity of velocity, shear stress, temperature and heat flux can be written as:

$$U_l = U_p\,,\ \mu_l \frac{\partial U_l}{\partial r}\bigg)_e = \mu_e \frac{\partial U_p}{\partial r}\bigg)_e \tag{14}$$

$$T_l = T_p\,,\ \lambda_l \frac{\partial T_l}{\partial r}\bigg)_e = \lambda_e \frac{\partial T_p}{\partial r}\bigg)_e \tag{15}$$

At the external face of the wall ($r = R'$), the conditions of no-slip and isothermal wall are imposed using:

$$U_p = 0, \quad T_p = T_w \tag{16}$$

Moreover, in order to write the equations in dimensionless form, the following reduced variables are introduced:

$$\left(r^*,\ \mathrm{z}^*,\ \delta^*\right) = \frac{\left(r,\ \mathrm{z},\ \delta\right)}{R} \tag{17}$$

$$\left(U_k^*,\ V_k^*\right) = \frac{\left(U_k\,,\ V_k\right)}{\sqrt{gR}}\,,\ T_k^* = \frac{T_k - T_w}{T_0 - T_w} \tag{18}$$

$$P^* = \frac{P - P_0}{\rho_0 g R}\,,\ q_k^* = \frac{q_k}{\mu_0 R} \tag{19}$$

The dimensionless groups resulting from this transformation are: e^*, Re_0, Fr, Pr_L, Pr_g, Sc, Ja, Da (defined in nomenclature) and the ratios of fluids properties:

$$\rho^* = \rho_g / \rho_l\,,\ \mu^* = \mu_g / \mu_l \tag{20}$$

$$\lambda^* = \lambda_g / \lambda_l\,,\ c_p^* = \left(c_{pv} - c_{pa}\right) / c_{pg} \tag{21}$$

$$\mu_e^* = \mu_e / \mu_l\,,\ \lambda_e^* = \lambda_e / \lambda_l \tag{22}$$

IV. Numerical Method

In this problem, the thickness of the liquid film is unknown and variable along the flow. To locate precisely the liquid-mixture interface, the following coordinate transformation is performed:

In the mixture ($0 \le r \le R-\delta$):

$$\eta_g = \frac{r}{R - \delta} \tag{23}$$

In the liquid film ($R-\delta \le r \le R$):

$$\eta_L = 2 + \frac{r - R}{\delta} \tag{24}$$

In the porous layer ($R \le r \le R+e$):

$$\eta_p = 2 + \frac{r - R}{e} \tag{25}$$

In this new referential, the porous, liquid and mixture phases are respectively defined in the ranges:

$$0 \le \eta_g \le 1,\ 1 \le \eta_l \le 2,\ 2 \le \eta_p \le 3$$

The transfer equations (1)–(7) and the associate boundary conditions (8)–(16) are rewritten in this new coordinate system and discretized by an implicit finite difference method. The space derivative terms are approximated by a backward difference scheme in the main flow direction and a central difference scheme in the radial direction. Systems of algebraic equations are then obtained for each variable (U_k, T_k, C) and solved successively line by line, using Gauss algorithm (for the momentum conservation equations) and Thomas algorithm (for heat and diffusion equations). The liquid film thickness at each axial location is calculated by the secant method using the mass balance equation at the liquid-mixture interface.

The discretization grid used in this work is uniform in the radial direction with three different grid spacings corresponding to each region ($\Delta\eta_g$ in the mixture, $\Delta\eta_l$ in the liquid film and $\Delta\eta_p$ in the porous coating), but non uniform along the streamwise direction. Indeed, in order to capture the rapid evolution of profiles near the tube inlet, on a short distance, the grid may start with a fine step size Δz. On the remaining length, the grid is then usually coarse with a larger step size.

In addition, a preliminary study of the effect of the number of nodes was conducted in order to determine the optimum mesh size. Calculations were performed for typical conditions indicated in section VI, with several grid distributions. For each grid size, the value of the average Nusselt number Nu is calculated and compared with that of the finest one. Table I shows the variations of Nu with the number of nodes along the radial direction (N_g in the mixture, N_l in the liquid film, N_p in the porous layer) and the axial direction (M near the leading edge, M' in the second part of the vertical axis z). It was found that a grid with (N_g = 28, N_l = 10, N_p= 10, M= 40, M' = 2380) produced relative error less than 1 %. So it was selected as the standard grid for further calculations.

Moreover, the numerical model and the computer code were validated by a comparison between the numerical and analytical results obtained after complete condensation. Indeed, during the condensation process of vapor-gas mixtures, the vapor mass fraction and the temperature decrease gradually. After a sufficient distance downstream from the inlet, the temperature of the whole domain becomes uniform and almost equal to that of the cooled wall. This state corresponding to the end of condensation has been highlighted by Siow et al. in the case of film condensation from vapor-gas mixtures

in a channel [10]. The final mass flow rate of condensate can then be determined from simple mass balances between the inlet and the end of condensation, as follows:

$$q_{cf} = q_{p0} + \left(\frac{C_0 - C_f}{1 - C_f} \right) q_{g0} \qquad (26)$$

The results from the analytical solution given by this relation and the numerical calculation for a wide range of various parameters are summarized in Table II. In all cases, these comparisons produced good agreements, since the relative error is less than 2.6 %.

TABLE I
AVERAGE NUSSELT NUMBERS FOR DIFFERENT GRID SIZES

M, M'	20, 1190	40, 2380	80, 4760
N_g, N_l, N_p			
20, 10, 10	7.531	7.556	7.584
28, 10, 10	7.613	7.632	7.659
40, 10, 10	7.663	7.692	7.705
28, 20, 20	7.603	7.629	7.650
40, 20, 20	7.670	7.701	7.708

TABLE II
EFFECT OF MAIN PARAMETERS ON THE CONDENSATE FLOW RATE AT THE END OF CONDENSATION

	Analytical results	Numerical results	Maximum relative error
Da = 10^{-6}, 10^{-5}, 10^{-4}, 10^{-3}	1430, 1621, 1815, 1854	1400, 1589, 1790, 1847	2.1 %
e^* = 0.0025, 0.005, 0.01, 0.015	1444, 1815, 4002, 7791	1406, 1790, 3997, 7788	2.6 %
C_0 = 0.7, 0.8, 0.9, 0.95	1108, 1336, 1639, 1815	1080, 1302, 1610, 1790	2.5 %
Re_0 = 250, 500, 1000, 2000	767, 1117, 1815, 3213	758, 1104, 1790, 3130	2.6 %

V. Solution Procedure

The solution procedure is summarized as follows:

1. At the inlet of the tube, the profiles of variables are initialized according to the inlet conditions for the porous layer and the mixture.
2. At the first axial station, inlet profiles are used as the initial guess for the values of variables.
3. An arbitrary value δ_1 of the film thickness is assumed for the station j.
4. The equations of momentum, continuity, heat in the three phases and mass diffusion in the mixture are sequentially solved using Gauss and Thomas algorithms.
5. The convergence test used is $E < 10^{-6}$, where E is the relative change of each variable (U_k, V_k, T_k, C), between two successive iterations. If the above criterion is verified for each node, then the solution convergence is declared and we move to the next step. Otherwise, the steps 4, 5 are repeated.
6. Another arbitrary value δ_2 of the film thickness is imposed and the steps 4, 5 are repeated until convergence.
7. The relative error E' on the liquid mass flow rate is calculated. If $E' > 10^{-6}$, then a better value of δ is calculated using the secant method and the steps 4, 5 are repeated until convergence. Otherwise, the last obtained value of δ is retained and the calculations are advanced in the streamwise direction.
8. Steps 3-7 are repeated for the next station.
9. Calculations are stopped when the end of the tube is reached.

VI. Results and Discussion

In this work, we consider a saturated steam-air mixture flowing in a vertical tube. Condensation occurs at the cooled wall which is coated with a thin porous layer. Calculations were first performed for the following conditions:

Porous layer: $e^* = 0.005$, $F = 0.55$, $\varepsilon = 0.5$, $\lambda_e^* = 1$, $\mu_e^* = 1$, $Da = 10^{-4}$.

Mixture: P_0 = 1 atm, C_0=0.95, Re_0 = 1000, Ja = 0.0184.

These values of C_0 and Ja correspond to T_0 = 99.2°C and $\Delta T = T_0 - T_w$ = 10 °C. The results are presented in dimensionless form. They include the distributions of velocity, temperature and vapor mass fraction as well as the evolutions of the liquid film thickness, mass flow rate of condensate, heat flux and pressure gradient.

VI.1. Detailed Profiles

Fig. 2 shows the dimensionless profiles of axial velocity in the three phases at various sections until the end of condensation. The mixture enters the tube at a uniform velocity U^* = 3.27. At the leading edge, high gradients of velocity appear at the liquid-mixture interface, leading to a gradual deformation of velocity profiles along the tube. From a distance z^* = 20, they tend to an almost parabolic shape for the mixture with a maximum velocity at the axis of the tube. During the flow, the decrease in the mixture velocity is accompanied by a significant increase in the condensate velocity in the liquid film and the porous layer, under the simultaneous effects of mass absorption by condensation from vapor and gravitational acceleration. The velocity of the condensate in the porous layer remains lower than that of the liquid film.

From the section z^* = 60, the velocity profiles remain invariant. The steady state corresponding to the hydrodynamic fully-developed conditions is then almost reached. The flows of both phases are laminar throughout the tube, since Reynolds numbers are sufficiently low (Re_g = 136 and Re_l = 12.7 at the end of the tube).

The dimensionless distributions of temperature in the three phases and vapor concentration in the mixture are shown in Figs. 3 and 4. These profiles are assumed uniform at the inlet. They are then submitted to a sudden drop at the wall.

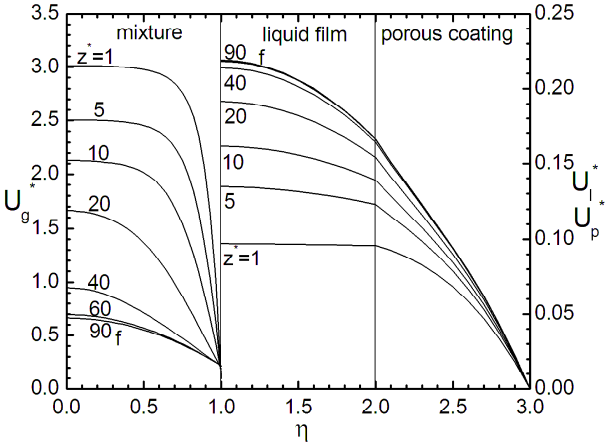

Fig. 2. Dimensionless velocity profiles at various sections

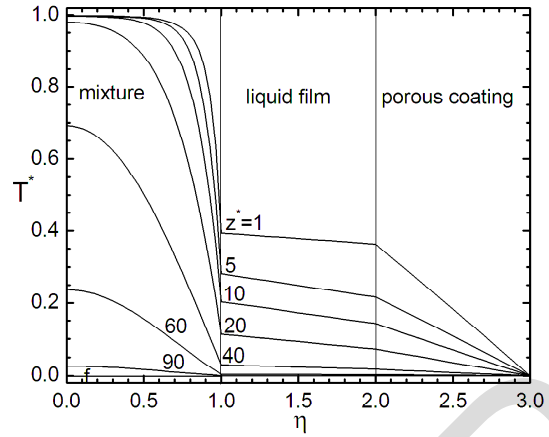

Fig. 3. Dimensionless temperature profiles at various sections

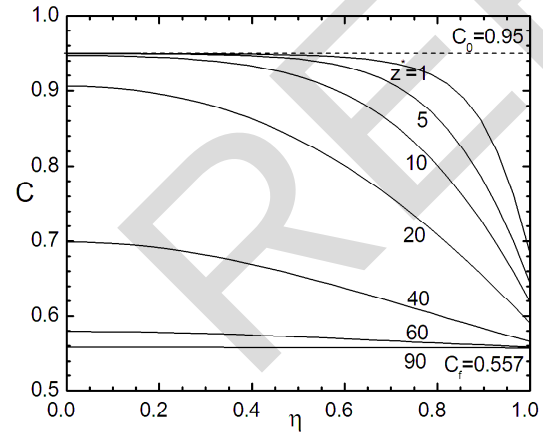

Fig. 4. Dimensionless vapor mass fraction profiles at various sections

It follows a progressive decrease of these quantities along the tube, leading to a continuous decrease in the rate of condensation. During the flow, profiles of temperature and concentration have a similar shape in the mixture. They remain maximal on the axis of symmetry of the tube and decrease until the liquid-mixture interface. In the liquid film and the porous layer, temperature variations are much smaller and the profiles are almost linear. Because of low condensate velocity and small thickness of porous layer, the effect of convective terms in these phases is negligible.

The thermal and mass profiles tend progressively to uniform values which are in fact the wall temperature and the final vapor concentration (C_f = 0.557). This state corresponds to the end of condensation which is almost reached after a distance z^* = 60.

VI.2. Condensate and Pressure Gradient

Fig. 5 shows the evolution of the liquid film thickness and the mass flow rate of condensate. We found that their values increase quickly near the inlet of the tube, due to the high concentration gradient in this region. Then they converge closely to limit values δ_f^* = 0.0033, and q_{cf}^* = 1790 corresponding to the complete condensation, after a distance z^* = 60 downstream from the inlet. The final thickness of the liquid film remains lower than that of the porous layer.

Fig. 6 shows the evolution of the axial pressure gradient and the dimensionless pressure.

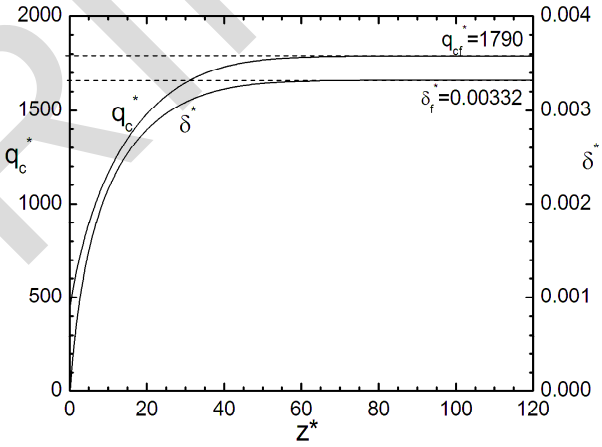

Fig. 5. Evolutions of mass flow rate of condensate and film thickness

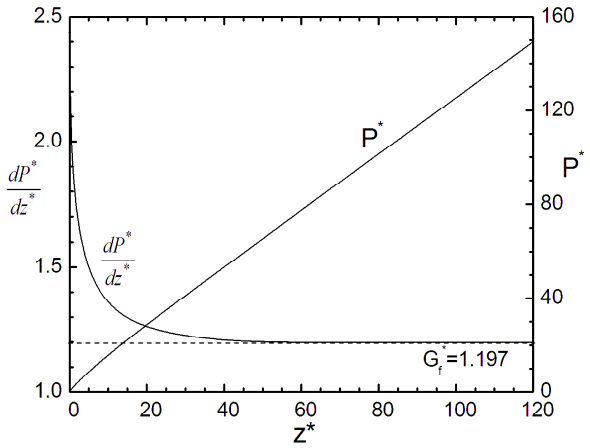

Fig. 6. Evolutions of dimensionless pressure and axial pressure gradient

The variation of the pressure gradient is significant near the inlet of the tube, and approaches a constant value at $z^* = 60$, corresponding to the end of condensation.

However, at the end of the tube, the relative increase in pressure is very small (about 0.01 % compared to the inlet pressure $P_0 = 1$ atm). The total pressure in the whole domain can then be considered nearly constant during the condensation process.

VI.3. Parametric Study

We present here a study of the effect of some important factors on the condensation process for a saturated steam-air mixture. The following parameters are maintained constant: $e^*=0.005$, $\mu_e^*=1$, $\lambda_e^*=1$. The end of condensation is considered achieved when the axial variation of all variables (except pressure) becomes practically zero. It is obtained for various lengths of the tube depending on the values of the parameters. Table II shows the analytical and numerical values of the final flow rate of condensate for various parameters at the end of condensation.

Figs. 7-8 show the effect of Darcy number (which is proportional to the permeability K of the porous layer) and the thickness of porous coating on the evolutions of condensate flow rate and heat flux. Calculations were performed separately for $0.0025 \le e^* \le 0.015$ and $10^{-6} \le Da \le 10^{-3}$. For a tube of radius $R = 1$ cm, these values correspond to a range 10^{-10} m$^2 \le K \le 10^{-7}$ m^2.

The results show that an increase in the porous thickness or Darcy number is accompanied by a net increase in the total flow rate of condensate. These properties directly affect the hydrodynamic behavior of the porous medium. Indeed, the intrinsic permeability characterizes the ability of material to enable the liquid infiltration and the thickness enhances the volume of internal pore in which fluid flow occurs. Both properties have the effect of enhancing the liquid transfer through the porous network.

Moreover, it was found that that an increase of the permeability has little effect on heat transfer characteristics. An increase of Da from 10^{-6} to 10^{-3} leads to an increase in heat flux of only 3.8 % under the prescribed conditions. Similar trends were found with the previous results of Renken et al. [4] about of the effect of Darcy number on the forced convective condensation of saturated vapor on a vertical plate coated with a thin porous layer.

By analyzing the influence of the thickness of porous layer, we note that an increase of e^* from 0.0025 to 0.015 leads to a significant increase in the values of total heat flux (about 21.4 %) for the conditions specified. However, this study was limited to low values of thickness, in order to verify the last assumption mentioned in the physical model. Indeed, further calculations showed that thicker porous layers are not totally covered by the condensate.

Therefore, a more complicated problem arises concerning vapor condensation inside a porous medium, for which our mathematical model is no longer valid.

Furthermore, the effect of inlet vapor concentration C_0 on the condensation process is shown in Fig. 9. Calculations were performed for C_0 varying between 0.7 and 0.95 (corresponding to saturation temperatures T_0 between 93.6°C and 99.2 °C).

With increasing C_0, the gradient of vapor concentration at the liquid-mixture interface increases significantly. Therefore, it leads to a high augmentation in the rate of condensation, and hence in condensate flow rate at any section of the tube. Fig. 9 also shows that the vapor concentration have a strong influence on the evolution of heat flux. Indeed, thermal gradients in the porous layer increase with C_0, leading to higher heat flux at the wall.

From $C_0 = 0.7$ to 0.95, the increase is 71 % for flow rate of condensate and 69 % for heat flux at the end of the tube. Similarly, Fig. 10 represents the effect of input Reynolds number of the mixture, for Re_0 varying between 250 and 2000. All other parameters are maintained constant.

Results show that the condensate flow rate increases strongly with Re_0. In fact, higher Re_0 leads to increase vapor flow rate. Hence more steam is available to condense and contributes to enhance the film thickness and the condensate flow rate. As the initial and final vapor concentrations are maintained constant, the final mass flow rate of condensate is almost proportional to Re_0. The same figure represents the axial evolution of the dimensionless heat flux at the wall. It shows clearly that the heat flux increases highly with Re_0, due to the increased thermal gradients in the porous substrate and temperatures at the liquid-porous layer interface.

Finally, from Figs. 7-10, it is easily seen that the tube length required for complete condensation increases highly with inlet Reynolds number and inlet gas mass fraction, while it is not significantly affected by Darcy number and thickness of porous layer.

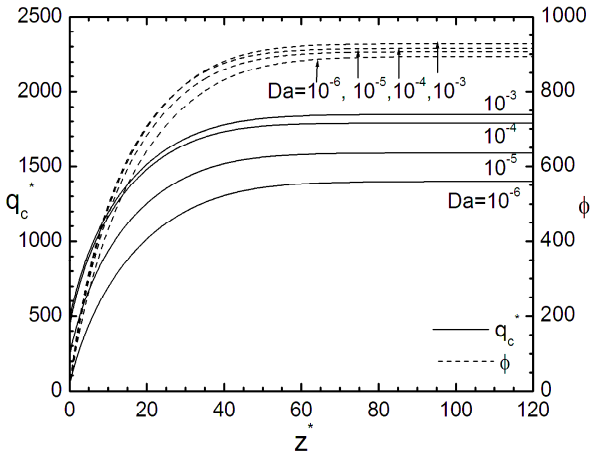

Fig. 7. Effect of Darcy number on the condensate flow rate and heat flux

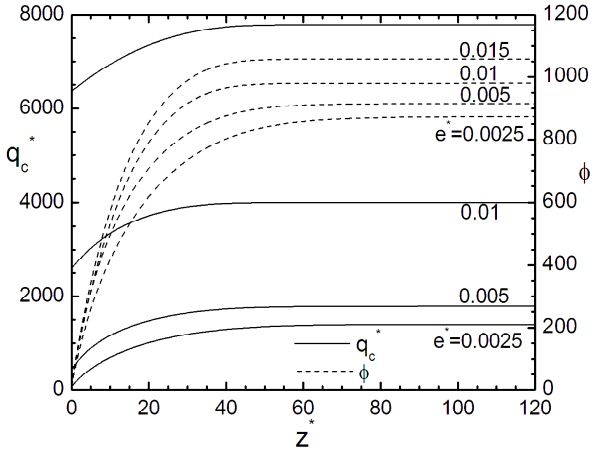

Fig. 8. Effect of thickness of porous layer on the condensate flow rate and heat flux

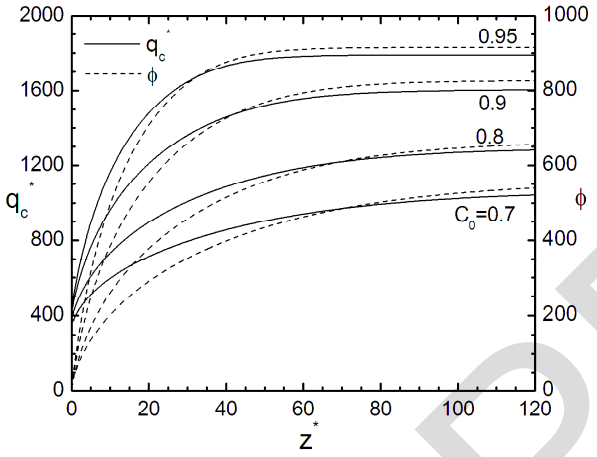

Fig. 9. Effect of inlet vapor mass fraction on the condensate flow rate and heat flux

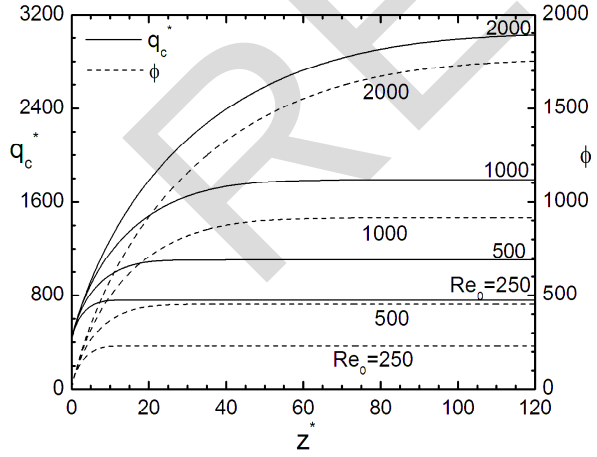

Fig. 10. Effect of inlet Reynolds number on the condensate flow rate and heat flux

VII. Conclusion

A numerical investigation was performed to study the process of laminar film condensation from steam-air mixtures on the porous wall of a vertical tube. Transfers in the steam-air mixture and the liquid film are described by the complete boundary layer equations. The flow in the porous layer is described by the Darcy-Brinkman-Forchheimer model. An implicit finite difference scheme has been used to solve the dimensionless equations. Calculations were performed for low values of porous layer thickness and a wide range of independent parameters. Detailed numerical results were obtained including profiles of velocity, temperature and vapor mass fraction from the tube inlet until the complete condensation. Moreover, axial evolutions of the film thickness, condensate mass flow rate and heat flux are also presented. The effects of some important parameters of the porous layer and the mixture are investigated. It was found that the wall heat flux increases significantly with the thickness of porous layer, inlet Reynolds number and inlet vapor concentration. However, it is little affected by Darcy number. The condensate flow rate increases highly with permeability, thickness of porous layer and inlet properties of the mixture. However, a more extensive study should be performed in order to investigate the effect of other important parameters such as inlet pressure, Jakob number, effective thermal conductivity and high values of porous coating thickness. The model may also be modified to turbulent mixture flow.

References

[1] W. Nusselt, The condensation of steam on cooled surfaces (Traduit par D. Fullarton), *Zeitschrift des Vereines Deutscher Ingenieure*, *Vol . 60*, n. 27, pp. 541-575, 1916.

[2] A. Shekarriz, O.A. Plumb, Enhancement of film condensation using porous fins, *Journal Of Thermophysics and Heat Transfer, Vol. 3*, n. 3, pp. 309-314, 1989.

[3] K.J. Renken, D.J. Soltykiwicz, D. Poulikakos, A study of laminar film condensation on a vertical surface with a porous coating, *International Communications in Heat and Mass Transfer, Vol. 16*, n.2, pp.181-192, 1989.

[4] K.J. Renken, M.J. Carneiro, K. Meechan, Analysis of laminar forced convective condensation within thin porous coatings, *Journal of Thermophysics and Heat Transfer, Vol. 8*, n. 2, pp. 303-308, 1994.

[5] K. J. Renken, M. R. Raich, Forced convection steam condensation experiments within thin porous coatings, *International Journal of Heat and Mass Transfer, Vol. 39*, n. 14, pp. 2937-2945, 1996.

[6] X. Ma, B. Wang, Film condensation heat transfer on a vertical porous-layer coated plate, *Science in China (Series E)*, *Vol. 41*, n. 2, pp.169-175, 1998.

[7] M. Asbik, R. Chaynane, H. Boushaba, B. Zeghmati, A. Khmou, Analytical investigation of forced convection film condensation on a vertical porous-layer coated surface, *Heat and Mass Transfer*, *Vol. 40*, pp. 143–155, 2003.

[8] R. Chaynane, M. Asbik, H. Boushaba, B. Zeghmati, A. Khmou, Etude de la condensation en film laminaire d'une vapeur pure et saturée sur la paroi poreuse d'une plaque inclinée, *Mécanique & Industries*, *Vol. 5*, n. 4, pp. 381-391, 2004.

[9] M. Asbik, B. Zeghmati, H. Gualous-Louahlia, W. M. Yan, The effect of thermal dispersion on free convection film condensation